Journal of Marine Research, 58, 631–651, 2000

The influence of deposit-feeding on chlorophyll-*a* degradation in coastal marine sediments

By Anitra E. Ingalls[1], Robert C. Aller[1], Cindy Lee[1] and Ming-Yi Sun[2]

ABSTRACT

To determine how macrofaunal activity affects rates and mechanisms of Chlorophyll-*a* (Chl-*a*) decomposition, we measured Chl-*a* concentrations during laboratory incubations of surface sediment with varying abundances of a subsurface deposit-feeder, ***Yoldia limatula.*** Decomposition patterns of Chl-*a* in sediment cores with and without a layer of algal-enriched sediment added to the surface were compared. Decomposition rate constants, k_d, were calculated from the loss of reactive Chl-*a* and further quantified using a nonsteady state, depth-dependent, reaction-diffusion model. Values of k_d decreased approximately exponentially with depth and were directly proportional to the number of ***Yoldia*** present. ***Yoldia*** increased the k_d of both natural sedimentary Chl-*a* and algal enriched Chl-*a* in the upper 2 cm by up to 5.7×. Surface sediment porosity, penetration depths of a conservative tracer of diffusion (Br^-), and oxidized metabolic substrates (e.g. Fe(III)) all increased significantly in the presence of ***Yoldia.*** Macrofaunal bioturbation increased the importance of suboxic degradation pathways. These experiments demonstrated that organic compounds from a single source can have a continuum of degradation rate constants as a function of biogenically determined environmental conditions (Chl-*a* $k_d \sim 0.0043$–$0.20\ d^{-1}$). In particular, Chl-*a* can have a continuum of k_d values related to redox conditions, transport, and macrofauna abundance as a function of depth.

1. Introduction

In near-shore environments, the existence of high productivity, high sedimentation, shallow water depths and anoxic conditions often allow a relatively large fraction of fresh organic carbon from primary production to be preserved in sediments. As a consequence, coastal sediments, which comprise 10% of the ocean floor, store 80% of marine organic carbon (Berner, 1989; Hedges and Keil, 1995). The relative importance of anoxia in determining preservation patterns of organic compounds in sediments is frequently debated (e.g. Canfield, 1989; Lee, 1992; Cowie ***et al.,*** 1995; Andersen, 1996). The presence of aerobic infauna, particularly those capable of bioturbation, is a key consequence of oxic conditions (Wishner ***et al.,*** 1990) and is proposed to be an important control on organic carbon preservation in oxic and anoxic sediments (Andersen and Kristensen, 1992; Aller, 1994; Blair ***et al.,*** 1996; Pope ***et al.,*** 1996).

1. Marine Sciences Research Center, SUNY, Stony Brook, New York, 11794, U.S.A. ***email: aingalls@ic.sunysb.edu***

2. Department of Marine Sciences, University of Georgia, Athens, Georgia, 30602, U.S.A.

This study directly tests the hypothesis that infaunal activity promotes Chlorophyll-*a* (Chl-*a*) decomposition and, by inference, sedimentary organic carbon decomposition generally. We measured changes in reactive Chl-*a* pool size and decomposition rate constants in Long Island Sound sediments in incubations where the number of *Yoldia limatula* was varied. *Yoldia* is a tenticulate subsurface (occasionally surface) deposit-feeding bivalve capable of bioturbating the upper 2–4 cm of muddy sediment. It is commonly found in Long Island Sound (LIS) in abundances on the order of 300 m^{-2}. During feeding, large quantities of sediment are ingested; however, up to 95% of ingested sediment is ejected as pseudo-feces (Lopez and Levinton, 1987).

Chl-*a* is the most abundant photopigment in living phytoplankton, and while it is a minor cellular component, it is a particularly useful tracer of the fate of primary production derived organic carbon. In coastal bioturbated sediments, Chl-*a* degrades until background concentrations (usually <1.0 nmol/gdw) are reached, typically within the upper 5–10 cm (Sun *et al.,* 1991; 1994; Gerino *et al.,* 1998). Models of sediment Chl-*a* profiles and incubation experiments show that Chl-*a* has a half-life between 14–55 days under either anoxic or oxic conditions (Furlong and Carpenter, 1988; Bianchi and Findlay, 1991; Sun *et al.,* 1993a,b). Under anoxic conditions, while initial decomposition rates are similar to those under oxic conditions, the anoxically reactive pool of Chl-*a* is small (Sun *et al.,* 1993a,b). This results in higher eventual background concentrations in anoxic sediments in the laboratory (Sun *et al.,* 1993a) and in the field (Furlong and Carpenter, 1988; Hastings *et al.,* 1998).

Coastal sediments with oxygenated overlying waters have abundant infauna whose bioturbation activity transports sediment particles across the redox boundary ($\sim$2–3 mm). In laboratory incubation experiments, Chl-*a* that is occasionally exposed to free O_2 degrades faster and more completely than Chl-*a* maintained under anoxic conditions (Sun *et al.,* 1993a; Aller, 1994). While only the surface 2 mm of sediment in coastal regions is oxic, background concentrations of organic compounds preserved at depth in sediments are comparable to concentrations observed in oxic incubations of sediments in the laboratory (Sun *et al.,* 1993a,b). This observation, combined with the knowledge that organic carbon decomposition is dominated by anaerobic pathways (Jørgensen, 1982), suggests that periodic exposure to O_2 is an important mechanism for achieving low background concentrations of organic carbon. Recent laboratory and modeling studies show that bioturbation increases the contribution of anaerobic degradation by mixing reactive carbon into the suboxic zone, and by continually reoxidizing electron acceptors used during anaerobic metabolism (Mackin and Swider, 1989; Aller, 1990; Soetaert *et al.,* 1996). In this experiment, we also measured Br^-, Fe oxidation state, and O_2 to relate Chl-*a* decomposition to indicators of solute transport and oxygen dynamics.

2. Materials and methods

a. Sediment collection and experimental setup

Chl-*a* degradation was investigated using naturally occurring sedimentary Chl-*a* (experiment A) or Chl-*a* from freeze-dried algae (experiment B). Both experiments were carried

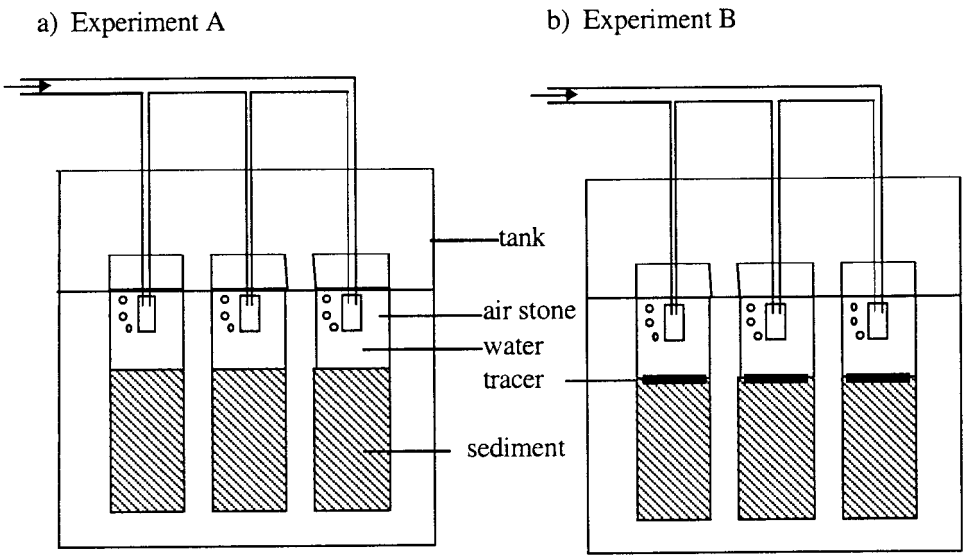

Figure 1. (a) Experiment A consisted of two treatments, I (no *Yoldia*) and II (3 *Yoldia*). No tracer cakes were added. (b) Experiment B consisted of four treatments, I (no *Yoldia*), II (1 *Yoldia*), III (3 *Yoldia*) and IV (5 *Yoldia*). Tracer cakes were added to all cores.

out using surface sediment (top 2 cm) from Long Island Sound Station P, the site of the LIS Pulse Study located in north central LIS (14 m water depth; Gerino *et al.,* 1998). Sediment was collected using a grab sampler on October 11, 1996 (experiment A) or March 13, 1997 (experiment B). The grab sampler collects approximately the upper 20 cm of sediment. The surface (brown porous) sediment was scraped off the deeper (gray or black, less porous) sediment with a spatula. Multiple grabs were performed until enough surface sediment was collected. In experiment A, the sediment was sieved (1 mm) and refrigerated for 10 days before the experiment was set up. Experiment B was set up immediately after sieving the sediment (1 mm). In both experiments, CAB (cellulose acetate butyrate) core tubes (7.4 cm inner diameter) were filled with homogenized sediment to a height of 10 cm. In experiment A, sediment containing naturally occurring Chl-*a* was incubated. In experiment B, each core received a simulated algal bloom input in the form of a 0.5-cm thick layer of sediment enriched with ^{13}C isotopically tagged-algae (the ^{13}C label was present for the purpose of investigating degradation of lipids; these results are reported elsewhere (Sun *et al.,* 1999). Cores were placed into tanks (3 or 4 cores per tank), and approximately 500 ml (12 cm) of filtered Long Island Sound water (collected at the same time as the sediment) was placed over the sediment. The tanks were filled with water to a height equal to the cores to prevent hydrostatic loss of water from the core tops, and to buffer changes in temperature. Each core was aerated using an aquarium aerator and air stone, and maintained at 20 $\pm$ 2°C (Fig. 1).

Each tank contained cores of the same *Yoldia* abundance or treatment (Table 1). *Yoldia* of 1.0–1.4 cm shell length were obtained from the Marine Biological Laboratory (Woods

Table 1. Experimental setup and sampling schedule.

Experiment	*Yoldia*	Tracer cake	$t = 1$ (days)	$t = 2$ (days)	$t = 3$ (days)	$t = 4$ (days)
A: I	0	no	—	6	15	27
A: II	3	no	—	6	15	27
B: I	0	yes	5	10	18	—
B: II	1	yes	5	10	18	—
B: III	3	yes	5	10	18	28
B: IV	5	yes	5	10	18	—

Hole, MA). One core was used to establish $t = 0$ conditions in all treatments in each experiment. The $t = 0$ core was sectioned immediately after being placed in a tank with overlying water. Experiment A was set up with two treatments; A: I (no *Yoldia*) and A: II (3 *Yoldia* per core). Experiment B was set up with 4 treatments; B: I (no *Yoldia*), B: II (1 *Yoldia* per core), B: III (3 *Yoldia* per core) and B: IV (5 *Yoldia* per core). *Yoldia* abundances used reflect the range found in Long Island Sound (1 *Yoldia*/core equals 200 animals/m^2). *Yoldia* that did not burrow below the sediment surface within 1 hour were removed and replaced with more active animals. Algal-enriched layers of sediment were added to the cores after all *Yoldia* burrowed below the core surface and generated turbidity in the overlying water (within 24 hours).

Approximately 24 hours prior to each sampling time, NaBr was added ($\Delta[Br^-] \sim 5$ mM) to the overlying water of one core in each treatment as a conservative tracer of pore water transport. The core was removed, sectioned (0.0–0.5 cm, 0.5–1.0 cm, 1.0–2.0 cm and 4 cm-bottom) and frozen. The overlying water was changed in each core every seven days to remove accumulated metabolites. Suspended sediment from cores with *Yoldia* was separated from the removed overlying water by centrifugation and returned to the core.

Algal-enriched cakes added to experiment B cores were prepared by adding 4.0 g of ground algae (^{13}C-labeled lyophilized *Chlorella* cells from Cambridge Isotope Labs) to 800 g wet sediment (1 mm sieved). The algae were hand mixed into the sediment for 30 minutes using a metal spatula. The sediment was formed into cakes (7.2 cm × 0.5 cm) and frozen and weighed before being placed on the cores.

b. Pigment analysis

Chl-*a* was extracted from thawed, homogenized subsamples of sediment core sections (approximately 1 g) using 5 ml HPLC grade 100% acetone (Sun *et al.,* 1991). The sediment slurry was mixed using a vortex stirrer, sonicated for 10 minutes while protected from light and centrifuged at 2,500 G for 5 minutes. The supernatant was collected and the identical extraction procedure was repeated on the disrupted pellet. The two extracts were combined and syringe-filtered through a 0.2 μm Zetapor membrane filter. Filtered extracts were stored in the dark at −15°C until HPLC analysis (<48 hours).

Chl-*a* and phaeophytin-*a* concentrations were determined by ion-pairing reverse-phase

high performance liquid chromatography (after Mantoura and Llewellyn, 1983). The HPLC system used was a Beckman Model 420 gradient controller with Beckman 110A pumps equipped with a 5 μm C-18 Adsorbosphere column (250 × 4.6 mm i.d.). Pigment detection was carried out with a Kratos FS 970 fluorometer (405 nm excitation and >580 nm emission). Resulting peaks were integrated using Shimadzu Class VP software. The primary eluant was a 20% aqueous solution of 0.5 mM tetrabutyl ammonium acetate and 10 mM ammonium acetate in methanol (A). The secondary eluant was 20% acetone in methanol (B). After injection of a 100 μl sample of pigment extract at room temperature, the gradient program ramped from 100% A to 100% B in 20 minutes at a flow rate of 1 ml/min. The column was then eluted with solvent B for 45 minutes.

The retention time of Chl-*a* was determined using an authentic standard (Sigma Chemical Company). The Chl-*a* standard was quantified spectrophotometrically (Hewlett Packard 8452 A Diode Array Spectrophotometer) in 90% acetone using an extinction coefficient of 68,700 at 440 nm (Mantoura and Llewellyn, 1983). Standards were run daily to track any drift in the fluorometer response. A phaeophytin-*a* standard was prepared by acidification of the Chl-*a* standard with HCl. Pigment concentrations are reported in nmol/g dry weight. Precision for replicate samples extracted over a several month period was ±3%. Extraction efficiencies for this technique have been reported previously and are 90.3 ± 3.1% of Chl-*a* added to wet sediment (Sun *et al.,* 1991).

c. Porosity, iron, bromide and O_2 analysis

Porosity was determined by weighing ~1 g of sediment before and after drying in a 60°C oven overnight, and assuming a density of 2.6 g/cm^3. Pore water samples (separated by centrifugation at 2500 g) were acidified to pH 2 using HCl and then frozen until analysis. Bromide was determined colorometrically by oxidation with chloramine-T in the presence of phenol red (Presley, 1971). Iron (solid phase) was determined on 6N HCl extracts (15 minutes) by the ferrozine method with (for Fe_R, total non-pyritic reactive Fe) and without (for non-pyritic Fe(II)) $NH_2OH \cdot HCl$ (Stookey, 1970; Aller *et al.,* 1996). Oxygen was measured with an oxygen microelectrode at the final sampling time. The electrode was calibrated using sea water bubbled with air (saturated) or N_2 (anoxic).

3. Results

a. Porosity and diffusive transport

All sediment incubations containing *Yoldia* demonstrated visible changes within the first few days. The overlying water became turbid, and the sediment water interface diffuse. Initial porosity was approximately 0.77 throughout the homogenized core. With *Yoldia,* porosity of the upper 0.5 cm increased to an average value of 0.83 during both experiments. Porosity decreased to 0.75 deeper (2–6 cm) in the core due to compaction (Table 2).

The presence of *Yoldia* resulted in an increase in the diffusive transport of dissolved solutes. Within two to three weeks after the start of each experiment, Br^- added prior to

Table 2. Average porosity for surface and deep sediment intervals from $t = 1$ to $t = 4$. Initial ($t = 0$) porosity in both experiments was 0.77 ± 0.01.

Depth	A: I	A: II	B: I	B: II	B: III	B: IV
0.0–0.5 cm	0.75 ± 0.01	0.86 ± 0.03	0.79 ± 0.01	0.82 ± 0.02	0.82 ± 0.02	0.83 ± 0.02
2–6 cm	0.80 ± 0.02	0.76 ± 0.02	0.75 ± 0.01	0.75 ± 0.01	0.75 ± 0.01	0.75 ± 0.01

sampling had a deeper penetration depth when *Yoldia* were present (Fig. 2a). Models of [Br^-] suggest that diffusive transport increases by 1.3–2.7× in the presence of *Yoldia* (Sun *et al.,* 1999). The increase in porosity (ρ) alone would have increased the flux of Br^- into the sediment by 1.1–1.3× (based on ratio of $(\rho)^2$ with and without *Yoldia*). O_2 penetration depth increased only ~0.5 mm with *Yoldia* present (Fig. 2b). Dissolved O_2 profiles were very similar in shape and magnitude in both cases. In contrast, the contribution of oxidized Fe increased in the presence of *Yoldia* in the upper 1 cm ($Fe(II)/Fe_R$) after 6 days of incubation (Fig. 2c).

b. Chlorophyll-a profiles

The activity of *Yoldia* resulted in more rapid and more extensive degradation of Chl-*a* in the upper 2 cm. Chl-*a* degradation was directly proportional to *Yoldia* abundance (Fig. 3a, b). Because of the high Chl-*a* concentration in the cake sediment, 50× more Chl-*a* was degraded in the surface 0.5 cm in experiment B than in experiment A. With 3 and 5 *Yoldia,* almost the entire Chl-*a* signal from the algal cake was degraded within 18 days. Chl-*a* concentration in the mixed zone (0.5 cm–4.0 cm) increased during the first 5 days of the experiment and subsequently decreased; below >2 cm the concentration was only slightly affected. Chl-*a* below 4 cm did not measurably degrade, except in treatment III, where the incubation lasted an additional 10 days (28 days total). Chl-*a* concentrations decreased with time in experiment A: II (no algal cake, 3 *Yoldia*) where Chl-*a* was quickly removed relative to initial concentrations, particularly near the surface, and B: III (algal cake, 3 *Yoldia*) where Chl-*a* concentrations were quickly lowered to nearly natural sediment concentrations (Fig. 4a,b).

c. Phaeophytin-a profiles

Chl-*a* to phaeophytin-*a* ratios in the 0.0–0.5 and 2–6 cm intervals decreased with time in all incubations (Fig. 5a, b). When no algal cakes were added (experiment A), the decrease was approximately uniform with depth in the absence of *Yoldia.* With *Yoldia* present, a much larger decrease in the Chl-*a*/phaeophytin-*a* ratio occurred. In experiment B profiles, the decrease in the Chl-*a*/phaeophytin-*a* ratio was proportional to *Yoldia* abundance. These profiles are dominated by the high Chl-*a* tracer signal, however, and are therefore not easily interpreted.

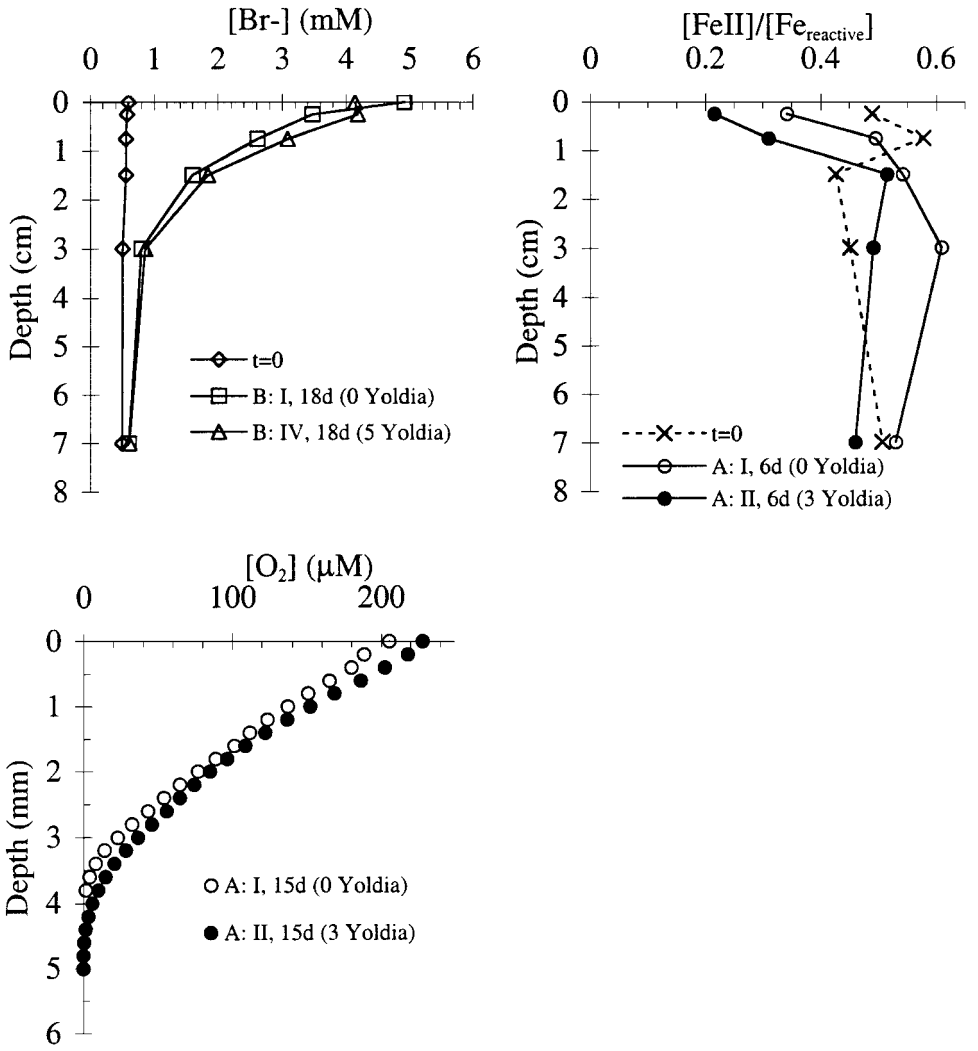

Figure 2. Examples of alteration of transport/redox conditions by *Yoldia.* (a) Pore water Br^- tracer profiles for experiment B (algal cakes, 18 days) I (0 *Yoldia*) and IV (5 *Yoldia*). Concentration at $x = 0$ is the overlying water concentration. (b) Pore water oxygen profiles from experiment A (no algal cakes added). (c) Fe(II)/Fe_R profiles in experiment A I (no cakes, 0 *Yoldia*) and A II (no cakes, 3 *Yoldia*) (see also Sun *et al.,* 1999; for additional examples).

4. Models

a. Chlorophyll-a decomposition rate model

The overall decomposition rate of Chl-*a* is approximately characterized by pseudo first-order kinetics (Sun *et al.,* 1991) as:

$$dI_r/dt = -k_d dI_r \tag{1}$$

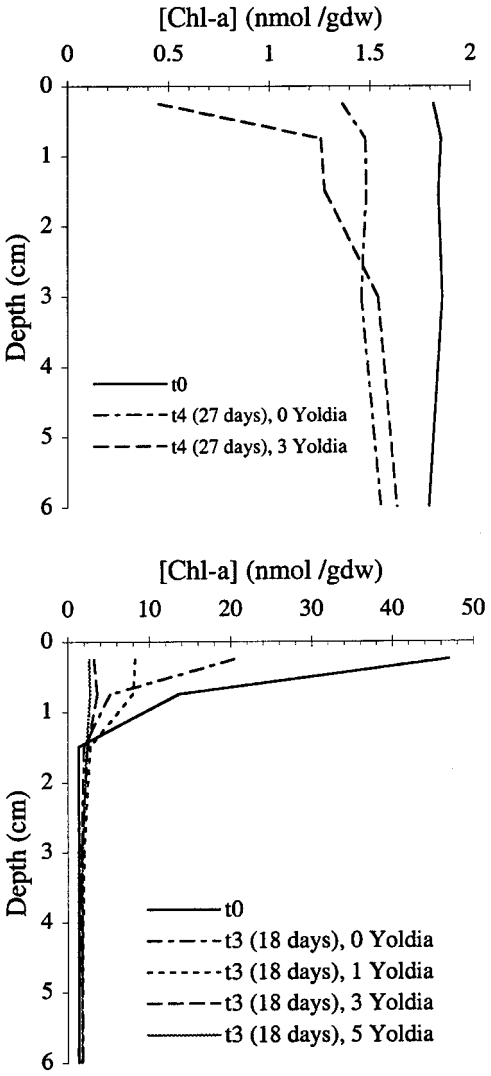

Figure 3. Initial and final Chl-*a* profiles of experiment A (a) and B (b).

I_r = reactive Chl-*a* inventory (nmol cm^{-2}) ($I - I_{\text{background}}$)
k_d = Chl-*a* decomposition rate constant (day^{-1})
The solution to Eq. (1) is:

$$I_r(t) = I_r(0) \exp(-k_d t) \tag{2}$$

where $I_r(0)$ is corrected for cake mass. $I_{\text{background}}$ is defined below.

Average decomposition rate constants for several depth intervals (0–0.5 cm, 0–2 cm, 2–6 cm and 0–6 cm) were calculated by fitting exponential curves (Eq. 2) to Chl-*a*

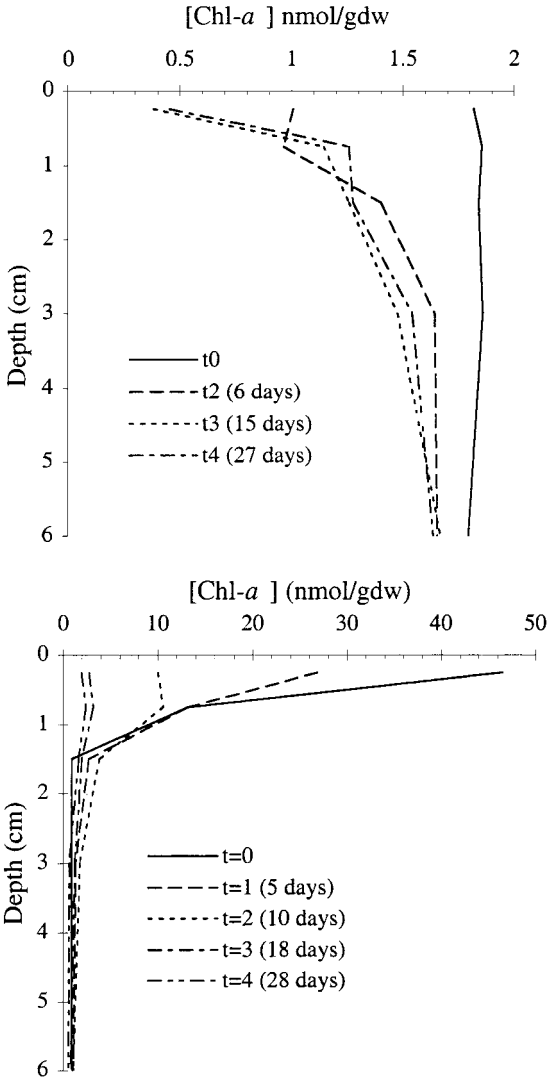

Figure 4. Chl-*a* profiles showing the change in concentration with time for treatments with 3 *Yoldia,* experiment A (a) and experiment B (b).

inventories (nmol/cm^2) (Table 3). The k_d calculated in the 0–2 cm interval represents the average $k_d(k_{avg})$ in the mixed layer (Fig. 6a, b). In experiment B (algal cakes added), the average k_d was modeled using the ratio of $I_r(t)/I_r(0)$ for each core due to differences in the mass of each algal cake. This ratio normalizes Chl-*a* inventory at any time to the amount of Chl-*a* present in each core at the start of the experiment. In order to give each measured point equal importance, the normalized exponential function was not forced through 1 at $t = 0$. Reactive Chl-*a* was defined as the amount of Chl-*a* in excess of background. For

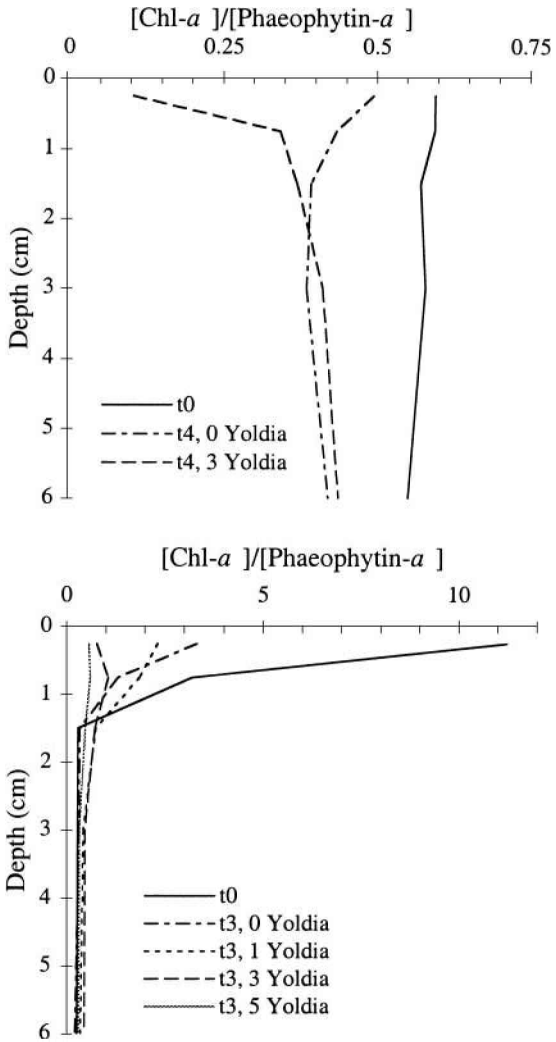

Figure 5. Chl-*a*/Phaeophytin-*a* ratios at initial and final sampling times for each treatment in experiment A (a) and experiment B (b).

these calculations, the potential minimum background inventory was considered to be the Chl-*a* inventory in the 0.0–0.5 cm interval of A: II (no cake, 3 *Yoldia*) at $t = 4$ (27 days), and was 0.061 nmol/cm^2 (0.5 nmol/gdw). This was the minimum Chl-*a* inventory observed in all experiments, and did not change significantly between 15 and 27 days. Background Chl-*a* was considered unavailable for decomposition with respect to the mechanisms acting in this experiment. Background Chl-*a* concentrations commonly found in Long Island Sound sediment cores (0–1 nmol/gdw) probably represent a refractory pool of Chl-*a* that typically escapes degradation (Sun *et al.,* 1991; 1994; Gerino *et al.,* 1998). In choosing

Table 3. Chl-*a* decomposition rate constants, k_d, in d^{-1} and r^2 values, (r^2), derived from first-order decomposition model fits to Chl-*a* inventory versus time (no mixing correction).

Treatment	0.0–0.5 cm	0–2 cm	2–6 cm	0–6 cm
A: I	0.024 (0.72)	0.011 (0.96)	0.0043 (0.30)	0.0056 (0.58)
A: II	0.21 (0.99)	0.063 (0.93)	0.0046 (0.98)	0.015 (0.92)
B: I	0.046 (0.90)	0.043 (0.90)	N/A	0.024 (0.82)
B: II	0.11 (0.85)	0.073 (0.74)	N/A	0.043 (0.56)
B: III	0.17 (0.99)	0.099 (0.99)	0.012 (0.27)	0.058 (0.98)
B: IV	0.28 (0.99)	0.11 (0.99)	N/A	0.053 (0.86)

a background inventory, we assumed that the Chl-*a* in excess of background would eventually degrade, given enough time.

Average apparent k_d values were calculated for different depth intervals because profile shapes indicated obvious depth-dependent decomposition (Table 3, Fig. 7). The sediment was separated into three zones: top layer (0.0–0.5 cm), entire mixed layer (0–2 cm), and unmixed layer (2–6 cm). In the presence of *Yoldia,* loss of Chl-*a* from the surface-most layer reflected both degradation and mixing into and from underlying regions. Values of k_d calculated in the 0.0–0.5 cm interval were significantly greater than those calculated for the 0–2 cm interval in all cases. Similarly, the 0–2 cm interval had a higher k_d than the 2–6 cm interval. Because the 0–2 cm interval represents approximately the whole mixed zone, the calculated average k_d is due only to decomposition. Values of k_d in the 0–6 cm interval without *Yoldia* (experiment A: 0.0056 d^{-1} and experiment B: 0.024 d^{-1}) were similar to rate constants for the decomposition of Chl-*a* previously observed in anoxic incubations (0.01 d^{-1}) and less than those in oxic (0.03–0.1 d^{-1}) incubations with no macrofauna (Sun *et al.,* 1993a,b; Leavitt and Carpenter, 1990; Bianchi and Findlay, 1991). The 0–6 cm k_d values in the presence of *Yoldia* (0.015–0.053 d^{-1}) were higher than without *Yoldia,* and were very similar to those observed under oxic conditions.

Rate constants for the decomposition of Chl-*a* in the upper 2 cm of sediment of all incubations (approximate mixed zone) were 1.6–5.7× faster in the presence of *Yoldia* relative to no *Yoldia* treatments, and were proportional to *Yoldia* abundance (Table 3). In the 0.0–0.5 cm depth interval, k_d increased by a factor of 2.4–8.8× with *Yoldia* present (Table 3). In the case of experiment B, these values are an overestimate of the true average k_d in the surface 0.5 cm because they do not account for loss from the layer due to downward mixing of the algal cake, and upward mixing of Chl-*a* depleted sediment. In experiment A, average k_d values may be underestimates due to mixing upward of sediment relatively rich in Chl-*a*. To refine these estimations, the results from this decomposition-rate model are incorporated into a non-steady-state depth-dependent decomposition-rate model (next section).

b. Non-steady-state depth-dependent decomposition rate model

Visual inspection of the Chl-*a* concentration profiles from incubations without algal cakes over time (Fig. 3a) demonstrates that the decomposition rate constant (k_d) is highest

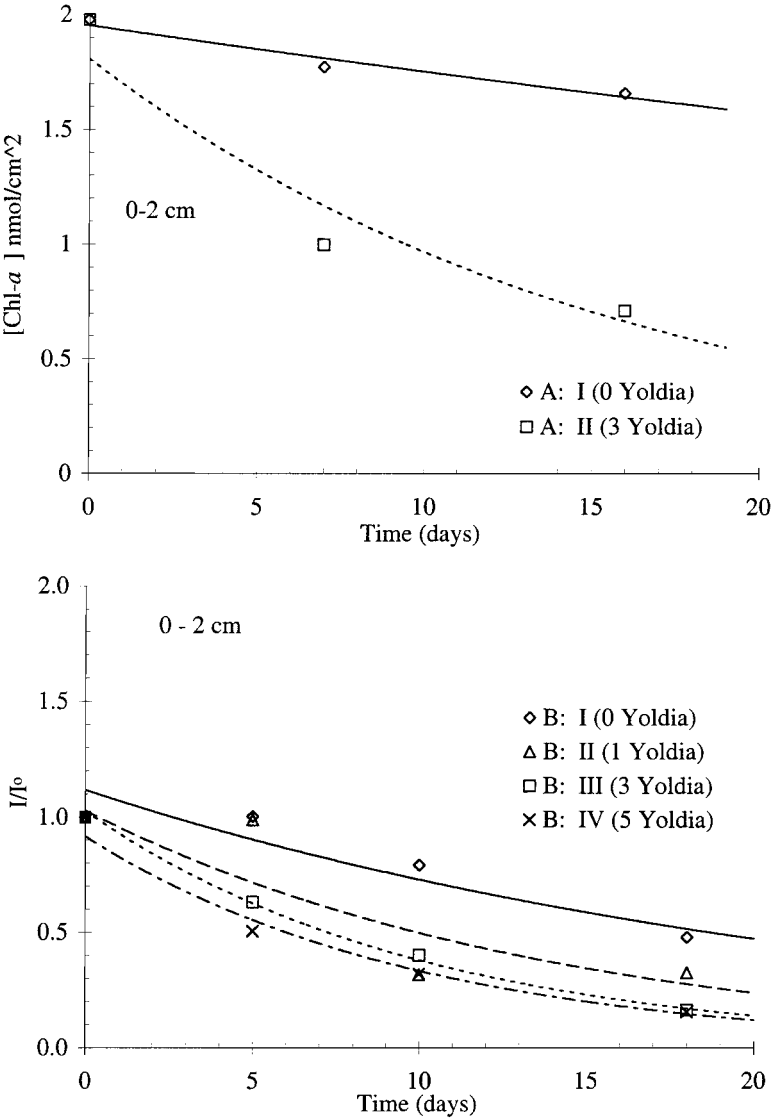

Figure 6. Chl-*a* inventory vs. time in the 0–2 cm depth interval in experiment A (a) and (b) experiment B (b): Decomposition rate constants were calculated by fitting an exponential function to the loss of Chl-*a* over time.

in surface sediment, and decreases with depth. Since the sediment is initially homogeneous, reactive Chl-*a* concentrations are initially equal throughout the core. At the conclusion of the experiment, concentrations are much lower at the surface than at depth. To better quantify the depth dependence of k_d, it is necessary to distinguish between changes in Chl-*a* concentration that are due to sediment mixing and those due to Chl-*a*

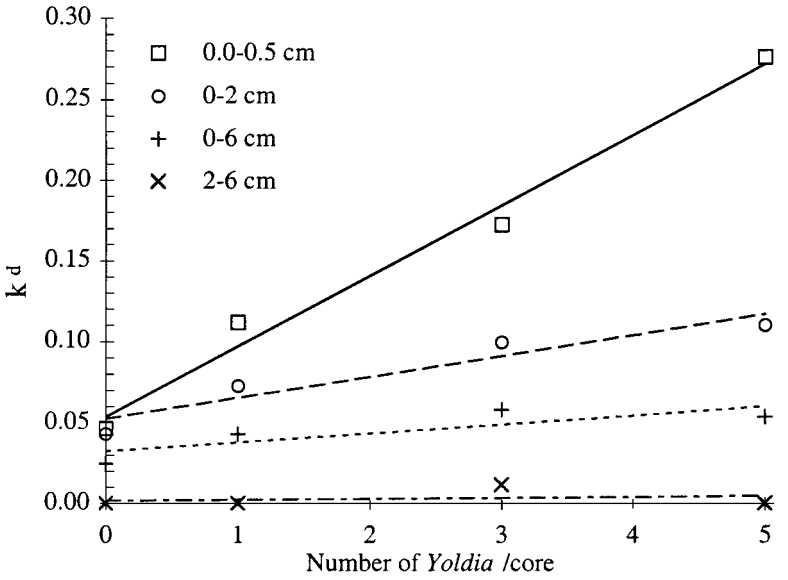

Figure 7. Comparison between k_d and *Yoldia* abundance for selected depth intervals. Slopes of linear fits are as follows: 2–6 cm = 0.0006; 0–6 cm = 0.0055; 0–2 cm = 0.013; 0.0–0.5 cm = 0.044. Exact calculation of k_d values in the surface 0.0–0.5 cm interval requires a correction for mixing of tracer in addition to decomposition.

decomposition. A plot of apparent k_d versus depth for experiment B (algal cakes added) suggests that $k_d \sim k_1 \exp(-\alpha x) + k_2$ is a reasonable functional form for approximating the depth dependence of k_d (Fig. 8). Sediment mixing by *Yoldia* is further approximated as diffusive. Chl-*a* concentration thus represents a balance between transport and reaction, and can be described by a steady-state depth-dependent reaction-diffusion model with an exponentially decreasing k_d in the mixed layer (top 2 cm). The vertical distributions of reactive Chl-*a* in the layer are given by:

$$C_t = D_B C_{xx} - k_1 e^{(\alpha x)} C - k_2 C \tag{3}$$

C_t = partial derivative of C with respect to time, t
C_{xx} = second partial derivative of C with respect to depth, x
k_1 = pre-exponential decomposition rate constant at $x = 0$ cm (day^{-1})
k_2 = asymptotic decomposition rate constant below the mixed layer ($x \sim 2$ cm) (day^{-1})
α = depth attenuation of k_d in the top 2 cm (cm^{-1})
D_B = biological mixing coefficient (cm^2 day^{-1}).
Initial conditions are:

$$C = C_T, \qquad 0 \le x \le L_1,$$

$$C = C_0 \qquad L_1 < x \le L_2$$

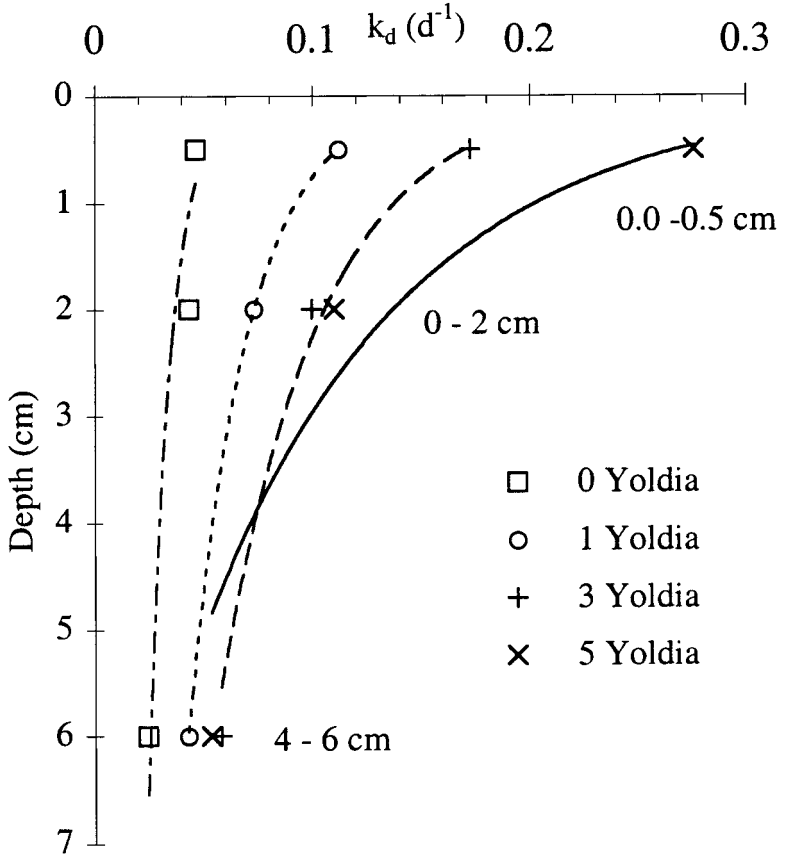

Figure 8. Relationship between k_d of Chl-*a* and depth interval for various *Yoldia* abundances in experiment B.

C_T = reactive Chl-*a* concentration at $L = 0$ and $t = 0$

C_o = reactive Chl-*a* concentration at the bottom of the mixed layer (generally ~2 cm) at $t = 0$

Boundary conditions are:

$$x = 0, \quad C_x = 0; \quad \text{(no flux across upper surface)}$$

$$x = L, \quad C_x = 0; \quad \text{(no flux into lower zone).}$$

L = mixed layer depth (2 cm)

L_1 = initial surface tracer layer (0.6–0.7 cm)

L_2 = unmixed layer (6.5 cm); midpoint of basal zone

C_x = first partial derivative of C with respect to depth, x.

The upper boundary condition ignores particle resuspension into overlying water during feeding by *Yoldia* (Sun *et al.,* 1999). Resuspension into oxic water is clearly an important

component of the decomposition process, but cannot be explicitly taken into account in the present case.

The model equations were solved numerically using a fully explicit, second-order finite difference scheme. The unknowns k_1, α, and D_B were assumed constant within a given treatment over the duration of the experiment. Estimates of k_1, α and D_B were calculated from the best model fit to Chl-*a* profiles using simultaneous constraints provided by profile shapes (3 averaged intervals/profile), time-dependence of profile shapes (3–4 time periods) and knowledge of the average decomposition rates in the mixed layer, 0–2 cm (average over experiment). The k_d for sedimentary Chl-*a* at the base of the mixed layer ($\sim k_2$) was first approximated as $\overline{k}_d$, the weighted average of k_d calculated for the 1–2 and 2–4 cm intervals in the A-I (no cakes, 0 *Yoldia*) and A-II (no cake, 3 *Yoldia*) treatments. This approximation assumes $k_1 \exp(-\alpha/L_1) \ll k_2$. Experiment A: I (0 *Yoldia*) had the same k_d value for both 1–2 and 2–4 cm intervals ($k_2 = 0.0075\ \mathrm{d}^{-1}$). In experiment A: II (3 *Yoldia*), k_d was $0.040\ \mathrm{d}^{-1}$ in the 1–2 cm interval, and $0.015\ \mathrm{d}^{-1}$ in the 2–4 cm interval. Thus, a k_2 of $0.023\ \mathrm{d}^{-1}$ was applied to calculations of cores with *Yoldia*. The values of k_2 calculated from experiment A were applied to model calculations of experiment B since decomposition of naturally present Chl-*a* could not be measured in this interval due to tracer cake derived Chl-*a* being mixed down by *Yoldia*. Applying k_2 values calculated from experiment A to the model of experiment B therefore assumes that decomposition at 2 cm (approximate depth of mixed layer) is the same with and without cakes, and with different *Yoldia* abundances. Due to differences in matrix, k_d of cake-derived Chl-*a* mixed down to 2 cm was probably higher than k_d of natural sedimentary Chl-*a* (Sun *et al.,* 1993b). To further constrain reaction rate variables, we can write an equation for $\overline{k}_d$ over the upper 2 cm.

$$\overline{k}_d = \frac{\int_0^2 (k_1 e^{-\alpha x} + k_2) C dx}{\int_0^2 C dx} \tag{4}$$

Eq. 4 insures that α, k_1 and k_2 are chosen such that the calculated $\overline{k}_d$ matches the weighted average k_d for the 0–2 cm interval (Table 3). Model parameters (k_1, α, D_B) were optimized to simultaneously minimize deviation of $\int C(x, t)$ from measured values over finite measurement intervals in single profiles, between successive profiles in a time series, and with measured $\overline{k}_d$. Uncertainties were computed as the standard deviation of optimal values estimated at different times in an experimental series.

Model results (Table 4) demonstrate that mixing coefficients and α both increased with an increase in the number of *Yoldia* per core. These differences are an indication that *Yoldia* had the greatest impact on surface sediment, intensifying the depth dependence of decomposition. No significant difference in α was observed between natural and cake derived Chl-*a* when *Yolida* were present (compare AII and BIII). This agreement indicates that *Yoldia* equalize the depth-dependence of the decomposition of Chl-*a* from different sources. Without *Yolida,* cake-derived Chl-*a* had a much smaller α, indicating that Chl-*a* in

Table 4. Nonsteady-state model values.

Treatment	k_1 (d^{-1})	k_2 (d^{-1})	α	D_B (cm^2/d)	$\overline{k}_d$
A: I	0.04 ± 0.02	0.0075	1.0 ± 0.4	0.000001	0.011
A: II	0.20 ± 0.06	0.023	1.3 ± 0.3	0.02 ± 0.01	0.0063
B: I	0.034 ± 0.006	0.0075	0.27 ± 0.06	0.0016 ± 0.0002	0.043
B: II	0.08 ± 0.06	0.023	0.90 ± 0.00	0.011 ± 0.002	0.073
B: III	0.14 ± .02	0.023	0.96 ± 0.08	0.015 ± 0.004	0.099
B: IV	0.19 ± 0.04	0.023	1.2 ± 0.0	0.021 ± 0.001	0.11

the cake was more uniformly reactive across the undisturbed redox boundary. This lack of depth dependence is expected because the added algae had been freeze-dried, and the cakes were frozen during preparation. Freezing can change the associations of Chl-*a*, resulting in more "free" Chl-*a* (Sun *et al.,* 1993a) which is highly reactive under anoxic conditions (Sun *et al.,* 1993b).

5. Discussion

a. Effects of Yoldia bioturbation on Chl-a degradation

Yoldia caused an increase in the rate and extent of degradation of Chl-*a*, and presumably of labile organic carbon. In previous experiments, periodic exposure of anoxic sediments to O_2 resulted in more thorough degradation of Chl-*a* (Sun *et al.,* 1993b; Aller, 1994). Redox oscillations can be important for organic carbon degradation because some organic compounds are not susceptible to anaerobic degradation mechanisms (Sun *et al.,* 1993b; Wakeham and Lee, 1993). However, if exposed to oxygen, alterations in the molecular structure or matrix may allow further degradation in the absence of free O_2 (Schink, 1988). Bioturbation transports sediment particles across redox boundaries. In our experiment, *Yoldia*-mediated "redox oscillations" appear to enhance the degradation of anoxically stable Chl-*a*, and changed the pathway of Chl-*a* degradation from anoxic to suboxic.

The increase in porosity that accompanied the addition of *Yoldia* is indicative of extensive bioturbation (Rhoads and Young, 1970). Models of Br^- distributions demonstrate that diffusive transport of dissolved solutes was increased 1.3–2.7× over that expected from changes in porosity alone (Fig. 2a; Sun *et al.,* 1999). Unlike Br^-, the increase in pore water O_2 penetration depth was negligible (Fig. 2b). Instead, additional O_2 diffusing into the sediment during mixing was consumed in reactions with reduced products of suboxic metabolism. For example, the fraction of reduced iron (Fe(II)) to Fe_R in surface sediment with three *Yoldia* was one half of that without *Yoldia* after only 6 days (top 0.5 cm interval) (Fig. 2c). Ammonium consumption also increased dramatically in surface sediment in the presence of *Yoldia,* indicating extensive nitrification, consistent with suboxic conditions (Sun *et al.,* 1999).

These changes indicate enhanced electron acceptor turnover and suboxic degradation in the presence of *Yoldia*. We did not measure the respiration of O_2 by *Yoldia;* however, other evidence indicates that macrofauna metabolic demand for molecular O_2 is a relatively

minor sink for O_2 in organic-rich deposits (Mackin and Swider, 1989; Andersen and Kristensen, 1992; Canfield *et al.,* 1993). More than half the O_2 that diffuses into organic-rich bioturbated sediments can be consumed in reactions with reduced sulfur, NH_4^+, Mn^{++} and Fe^{++} (e.g. Mackin and Swider, 1989; Aller, 1990; Canfield, 1993). Recent laboratory and modeling studies of early diagenesis confirm that bioturbation is one of the most powerful controls on the relative importance of oxic mineralization. Increased bioturbation results in rapid internal recycling of electron acceptors for anaerobic respiration, and therefore a greater anoxic and suboxic contribution to degradation (Aller, 1982; Kristensen, 1985; Aller, 1990; Soetaert *et al.,* 1996).

Evidence of differences in degradation pathway as well as decomposition rate are evident in profiles of Chl-*a* degradation products. For example, on the time scale of this experiment, phaeophytin-*a* is an expected stable primary degradation product of Chl-*a* in anoxic environments (Sun *et al.,* 1993a,b). When Chl-*a* degradation was observed in the anoxic zone (2–6 cm) of cores in experiment A, a similar increase in phaeophytin-*a* was seen. There was no increase in phaeophytin-*a* in the surface suboxic intervals in this experiment.

Direct ingestion of Chl-*a* by *Yoldia* may also affect degradation patterns. We think in this case, however, that direct ingestion is not the primary controlling factor. First, *Yoldia* feed subsurface, and degradation here was most intense at the surface interface. Second, there was no obvious delay in degradation rate such as might be expected due to the time necessary for surface material to reach the primary feeding zone. Third, depth dependence, although subdued, is still present in the absence of *Yoldia* (e.g. A: I).

b. Calculation of biological mixing coefficients

Previous studies demonstrate the usefulness of using Chl-*a* as an alternative to ^{234}Th as a tracer of biological mixing coefficients (Sun *et al.,* 1993, 1994; Gerino *et al.,* 1998). However, relatively small but significant differences between values of D_B calculated using ^{234}Th and Chl-*a* are typical (2–3×). One possible reason for the difference between these two tracers of mixing is that ^{234}Th has a well known and constant radioactive decomposition rate constant ($t_{1/2}$ = 24 days), while Chl-*a* degradation rate constants are dependent on a range of environmental factors, including temperature (Sun *et al.,* 1993a). Here we show that macrofauna can significantly influence the rate and depth dependence of Chl-*a* decomposition. Previously we used a constant k_d value calculated from a macrofauna-free incubation to model Chl-*a* flux to the sediment-water interface and biological mixing rates (Sun *et al.,* 1991, 1994; Gerino *et al.,* 1998). A more exact consideration of the effect of macrofauna may help improve this estimate.

c. Calculation of the flux of organic carbon

Since Chl-*a* is a component of organic matter produced during photosynthesis in surface waters, its behavior contains information about fluxes of primary-production-derived labile organic matter to the sediment-water interface. Sun *et al.* (1991; 1994) used Chl-*a* to

estimate the flux of labile organic carbon across the sediment water interface using two different methods. First, steady-state Chl-*a* concentration profiles and a laboratory derived decomposition rate constant were used to balance total supply and removal of Chl-*a* ($J = k_d I_r$). Alternatively, fluxes were estimated independently using biological mixing coefficients ($J = -D_B(\partial c/\partial x)$). If previous laboratory studies underestimate the k_d of Chl-*a* at the sediment water interface, the resulting organic carbon flux that is calculated will underestimate the true flux. Similarly, seasonal trends in bioturbation intensity will alter the flux calculated by these methods.

d. Relevance for organic carbon degradation

The size of the preserved pool of organic carbon in sediments is a function of the rate of degradation, the pool of carbon available for degradation and the length of time sediment is exposed to particular degradation mechanisms. This study shows that degradation is most rapid in the surface bioturbated zone, not necessarily because the material is inherently more labile, but because the environment at the surface promotes more extensive degradation (see Aller and Aller, 1998 for a review of solute transport affects on this result). In the natural environment, sedimentation eventually buries material below the bioturbated zone, limiting the length of time sediment remains in the zone were organic carbon is most susceptible to degradation. The amount of material buried then depends on the ratio of time that reactive material spends in the bioturbated zone, versus the half-life of the reactive pool under conditions in the bioturbated zone. Sedimentation rate and the depth of mixing determine how long a particle spends in the bioturbated zone, and therefore, the extent of degradation there.

Westrich and Berner (1984) incubated sediment from Long Island Sound and found a first order rate constant of 0.024 d^{-1} for the degradation of the most labile fraction of organic carbon, and 0.002–0.003 d^{-1} for the less reactive fraction. Compared to these values, the present study confirms that Chl-*a* in the surface layer of bioturbated sediment is an extremely labile component of total organic carbon (0.20 ± 0.06 d^{-1}). However, like bulk organic carbon, Chl-*a* also has a fraction that degrades over the same time-scale as the more refractory component of organic carbon (0.0043 ± 0.0002 d^{-1}, Table 3).

The recognition that sediments contain organic carbon with a range of reactivities has led to new developments in modeling approaches. Both the multi-G (Westrich and Berner, 1984; Soetaert *et al.,* 1996) and the reactive continuum (Middelburg, 1989; Boudreau and Ruddick, 1991) class of models of organic carbon degradation incorporate the idea that organic material becomes less reactive as it is increasingly degraded and changes composition. The present experiment complicates the definition of reactivity by demonstrating very clearly that environment can be as important in determining "reactivity" as is organic carbon source, age, or composition. The fact that the cores incubated in this experiment contained homogenized surface sediment throughout the length of the incubated cores, yet showed variable reaction rates, demonstrates that a single organic compound in a uniform matrix can have a reactive continuum that is exclusively

environment dependent. In the case of Chl-*a*, these rates can span almost 2 orders of magnitude, and can be approximated by an exponentially decreasing decomposition rate constant that approaches an asymptotic value. The depth dependence observed here in experiment A is likely suppressed relative to what might be observed in nature because Chl-*a* in surface sediment is likely to be inherently more reactive than the background Chl-*a* at depth.

6. Conclusions

Measuring the rate of change in Chl-*a* profiles in controlled microcosms with time demonstrated a clear effect of macrofauna on the decomposition of pigments and sedimentary organic carbon. Addition of algal cakes to the microcosms allowed the observation of how macrofauna might influence degradation of labile organic carbon that falls to the sea floor during a phytoplankton bloom. In the present study *Yoldia limatula,* a deposit-feeding protobranch bivalve, significantly increased the rate and extent of Chl-*a* degradation. Chl-*a* decomposition rates in surface sediment were attenuated exponentially with depth. Interpreted as a first-order kinetic process, decomposition was altered by *Yoldia* through both an increase in reaction rate constants and an increase in the pool of Chl-*a* available for decomposition. The depth and time-dependent pattern of decomposition implied that direct ingestion was not the major factor controlling Chl-*a* loss, although it must have contributed. By modeling the decomposition rate of Chl-*a* at different depth intervals, Chl-*a* profiles were reproduced using a non-steady-state transport reaction model with an exponentially decreasing k_d and diffusive particle mixing. This study demonstrated that the rate and extent of decomposition of specific components of marine organic carbon are dependent on the sedimentary environment as well as the architectural matrix in which the component is present in the sediment.

This work also represents a refinement of the previously reported rate constants for Chl-*a* degradation that takes into consideration the effect of macrofauna. The range of rate constants observed for Chl-*a* in this experiment represents a more realistic continuum of rate constants for fresh Chl-*a* deposited at the sediment-water interface during a bloom which is subsequently buried by sediment and bioturbated by macrofauna.

In addition to quantifying the depth dependence of degradation under different mixing regimes, this model may also confirm new interpretations of profiles of reactive sedimentary components. For example, subsurface peaks in sediment properties have traditionally been thought to result from biogenic advection of a pulsed input of a property at the sediment surface, with subsequent preservation in deeper sediment layers. Sun *et al.* (1991) suggest, and experiment B demonstrates, that subsurface peaks can be generated after a pulsed deposition (e.g., such as occurs after an algal bloom) if the decomposition rate constant varies within the mixed layer such that decomposition at the very surface occurs faster than at depth, and on a time scale that does not allow the input signal to be homogenized by mixing.

Acknowledgments. We thank the captain and crew of the R. V. *Onrust,* B. Zielenski and M. Wiggins. M. Green, M. Lima and Z.-B. Zhu helped with sampling and laboratory analyses. This manuscript was greatly improved by the careful comments of two anonymous reviewers. This research was supported by a grant from the OCE Division of NSF to M.-Y. Sun, R. C. Aller and C. Lee. Contribution number 1198 from the Marine Sciences Research Center, SUNY Stony Brook.

REFERENCES

Aller, R. C. 1982. The effects of macrobenthos on chemical properties of marine sediment and overlying water, *in* Animal-Sediment Relations, P. L. McCall and M. J. S. Tevesz, eds., Plenum, NY, 53–102.

—— 1990. Bioturbation and manganese cycling in hemipelagic sediments. Trans. R. Soc. London, Ser. A., *331,* 51–68.

—— 1994. Bioturbation and remineralization of sedimentary organic matter: effects of redox oscillation. Chem. Geol., *114,* 331–345.

Aller, R. C. and J. Y. Aller. 1998. The effect of biogenic irrigation intensity and solute exchange on diagenetic reaction rates in marine sediments. J. Mar. Res., *56,* 1–32.

Aller, R. C., N. E. Blair, Q. Xia and P. D. Rude. 1996. Remineralization rates, recycling, and storage of carbon in Amazon shelf sediments. Cont. Shelf Res., *16,* 753–786.

Andersen, F. Ø. 1996. Fate of organic carbon added as diatom cells to oxic and anoxic marine sediment microcosms. Mar. Ecol. Prog. Ser., *134,* 225–233.

Andersen, F. Ø. and E. Kristensen. 1992. The importance of benthic macrofauna in decomposition of macroalgae in a coastal marine sediment. Limnol. Oceanogr., *37,* 1392–1403.

Berner, R. 1989. Biogeochemical cycles of carbon and sulfur and their effect on atmospheric oxygen over Phanerozoic time. Palaeoegeogr. Palaeoclimatol. Palaeoecol., *73,* 87–122.

Bianchi, T. S. and S. Findlay. 1991. Decomposition of Hudson estuary macrophytes: photosynthesis pigment transformation and decay constants. Estuaries, *14,* 65–73.

Blair, N. E., L. A. Levin, D. J. DeMaster and G. Plaia. 1996. The short term fate of fresh algal carbon in continental slope sediments. Limnol. Oceanogr., *41,* 1208–1219.

Boudreau, B. P. and B. R. Ruddick. 1991. On a reactive continuum representation of organic matter diagenesis. Amer. J. Sci., *291,* 507–538.

Canfield, D. E. 1989. Sulfate reduction and oxygen respiration in marine sediments: implications for organic carbon preservation in euxinic environments. Deep Sea Res., *36,* 121–138.

—— 1993. Organic matter oxidation in marine sediments, *in* Interactions of C, N, P, and S Biogeochemical Cycles and Global Change, R. Wollast, F. T. Mackenzie and I. Chou, eds., Springer, Berlin, 333–363.

Cowie, G. G., J. I. Hedges, F. G. Prahl and G. L. De Lange. 1995. Elementary and major biochemical changes across an oxidation front of a relict turbidite: an oxygen effect. Geochim. Cosmochim. Acta, *59,* 33–46.

Furlong, E. T. and R. Carpenter. 1988. Pigment preservation and remineralization in oxic coastal marine sediments. Geochim. Cosmochim. Acta, *52,* 78–99.

Gerino, M., R. C. Aller, C. Lee, J. K. Cochran, J. Y. Aller, M. A. Green and D. Hirschberg. 1998. Comparison of different tracers and methods used to quantify bioturbation during a spring bloom: 234-Thorium, luminophores and chlorophyll-*a*. Est. Coast. Shelf Sci., *46,* 531–547.

Hastings, D. W., J. Villanueva and S. E. Calvert. 1998. EOS, Transactions, American Geophysical Union, Abstract only. *79,* OS74.

Hedges, J. I. and R. G. Keil. 1995. Sedimentary organic matter preservation: an assessment and speculative synthesis. Mar. Chem., *49,* 81–115.

Jørgensen, B. B. 1982. Mineralization of organic matter in the sea bed—the role of sulphate reduction. Nature, *296,* 643–645.

Kristensen, E. 1985. Oxygen and inorganic nitrogen exchange in a *Nereis virens* (polychaeta) bioturbated sediment-water system. J. Coastal Res., *1,* 109–116.

Leavitt, P. R. and S. R. Carpenter. 1990. Aphotic pigment degradation in the hypolimnion: implications for sedimentation studies and paleolimnology. Limnol. Oceanogr., *35,* 520–534.

Lee, C. 1992. Controls on organic carbon preservation: the use of stratified water bodies to compare intrinsic rates of decomposition in oxic and anoxic systems. Geochim. Cosmochim. Acta, *56,* 3323–3335.

Lopez, G. R. and J. S. Levinton. 1987. Ecology of deposit feeding animals in marine sediments. Quart. Rev. Biol., *62,* 235–260.

Mackin, J. E. and K. T. Swider. 1989. Organic matter decomposition pathways and oxygen consumption in coastal marine sediments. J. Mar. Res., *47,* 681–716.

Mantoura, R. F. and C. A. Llewellyn. 1983. The rapid determination of algal chlorophyll and carotenoid pigments and their breakdown products in natural waters by reversed-phase high-performance liquid chromatography. Anal. Chim. Acta, *151,* 297–314.

Middelburg, J. J. 1989. A simple rate model for organic matter decomposition in marine sediments. Geochim. Cosmochim. Acta, *53,* 1577–1581.

Pope, R. H., D. J. Demaster, C. R. Smith and H. Seltmann Jr. 1996. Rapid bioturbation in equatorial Pacific sediments: evidence from excess ^{234}Th measurements. Deep Sea Res. II, *43,* 1339–1364.

Presley, B. J. 1971. Techniques for analyzing interstitial water samples. Part 1: Determination of selected minor and major inorganic constituents. Initial Rep. Deep Sea Drilling Project, *7,* 1749–1755.

Rhoads, D. D. and D. K. Young. 1970. The influence of deposit-feeding organisms on sediment stability and community trophic structure (Buzzards Bay, MA). J. Mar. Res., *28,* 150–178.

Schink, B. 1988. Principles and limits of anaerobic degradation: environmental and technological aspects, *in* Biology of Anaerobic Microorganisms, A. J. B. Zehnder, ed., Wiley, NY, 771–846.

Soetaert, K., P. M. J. Herman and J. J. Middelburg. 1996. A model of early diagenetic processes from the shelf to abyssal depths. Geochim. Cosmochim. Acta, *60,* 1019–1040.

Stookey, L. L. 1970. Ferrozine—a new spectrophotometric reagent for iron. Anal. Chem., *42,* 779–781.

Sun, M.-Y., R. C. Aller, and C. Lee. 1991. Early diagenesis of chlorophyll-*a* in Long Island Sound sediments: a measure of carbon flux and particle reworking. J. Mar. Res., *49,* 379–401.

—— 1994. Spatial and temporal distributions of sedimentary chloropigments as indicators of benthic processes in Long Island Sound. J. Mar. Res., *52,* 149–176.

Sun, M.-Y., R. C. Aller, C. Lee and S. G. Wakeham. 1999. Enhanced degradation of algal lipids by benthic macrofauna activity: effect of *Yoldia limatula.* J. Mar. Res., *57,* 775–804.

Sun, M.-Y., C. Lee and R. C. Aller. 1993a. Laboratory studies of oxic and anoxic degradation of chlorophyll-*a* in Long Island Sound sediments. Geochim. Cosmochim. Acta, *57,* 147–157.

—— 1993b. Anoxic and oxic degradation of ^{14}C-labeled chloropigments and a ^{14}C-labeled diatom in Long Island Sound sediments. Limnol. Oceanogr., *38,* 1438–1451.

Wakeham, S. G. and C. Lee. 1993. Production, transport and alteration of particulate organic matter in the marine water column, *in* Organic Geochemistry, M. H. Engel and S. A. Macko, eds., Plenum, NY, 145–169.

Westrich, J. T. and R. A. Berner. 1984. The role of sedimentary organic matter in bacterial sulfate reduction: the G-model tested. Limnol. Oceanogr., *29,* 236–249.

Wishner, K., L. Levin, M. Gowing and L. Mullineaux. 1990. Involvement of the oxygen minimum in benthic zonation of a deep seamount. Nature, *346,* 57–59.

Received: *21 January, 1999;* revised: *27 March, 2000.*